

# PROCEEDINGS OF SPIE

[SPIDigitalLibrary.org/conference-proceedings-of-spie](https://SPIDigitalLibrary.org/conference-proceedings-of-spie)

## Atom probe tomography using Extreme-Ultraviolet Light

Miaja-Avila, Luis, Chiaramonti, Ann, Caplins, Benjamin,  
Diercks, David, Gorman, Brian, et al.

Luis Miaja-Avila, Ann N. Chiaramonti, Benjamin W. Caplins, David R. Diercks, Brian P. Gorman, Norman A. Sanford, "Atom probe tomography using Extreme-Ultraviolet Light," Proc. SPIE 11325, Metrology, Inspection, and Process Control for Microlithography XXXIV, 113250A (20 March 2020); doi: 10.1117/12.2551898

**SPIE.**

Event: SPIE Advanced Lithography, 2020, San Jose, California, United States

# Atom Probe Tomography using Extreme-Ultraviolet Light

Luis Miaja-Avila<sup>a</sup>, Ann N. Chiaramonti<sup>a</sup>, Benjamin W. Caplins<sup>a</sup>, David R. Diercks<sup>b</sup>, Brian P. Gorman<sup>b</sup>, and Norman A. Sanford<sup>a</sup>

<sup>a</sup>National Institute of Standards and Technology, Boulder, CO, USA

<sup>b</sup>Colorado School of Mines, Golden, CO, USA

## ABSTRACT

We present a different approach to laser-assisted atom probe tomography, where instead of using a near-UV laser for inducing a thermal transient, we use an extreme-ultraviolet coherent light source to trigger field ion emission at the tip's apex. The use of extreme-ultraviolet photons in atom probe tomography opens the potential for an athermal field ionization pathway.

**Keywords:** Atom probe microscopy, extreme ultraviolet, high-harmonic generation

## 1. INTRODUCTION

Laser-pulsed atom probe tomography (LAPT) is a powerful tool for materials characterization due to its combination of high spatial resolution and analytical sensitivity. In idealized terms, LAPT is a method that deconstructs a specimen one atom at a time, counts and identifies the individual atoms that comprised the specimen, and generates an atom-by-atom 3D “reconstruction” of the specimen.<sup>1-3</sup>

In LAPT a sample material is shaped into a sharp specimen “tip” with an apex radius typically ranging from 10 – 50 nm. The tip is then held at cryogenic temperatures (20 K – 100 K) and electrically biased with a DC standing voltage under ultra-high vacuum conditions. The DC standing voltage is carefully chosen to be just below the threshold for field ion evaporation. Due to the high DC standing voltage and the small radius at the tip's apex, the electric field strength at the vacuum/tip interface is on the order of tens of V/nm. In state-of-the-art conventional laser atom probe, a pulsed, focused laser (typical wavelength 355 nm or 532 nm) is used to induce thermal transients that trigger controlled field ion evaporation from the tip. Each field evaporated ion is accelerated towards the detector where its time-of-flight (TOF) and impact position is recorded, see Figure 1. The identities of the ions are inferred from the TOF data and their origination location are extracted with back-projection algorithms. The accumulated dataset of TOF and origination position is then used to numerically generate a 3D “reconstruction” of the specimen.

LAPT has been used to study a variety of materials, spanning from metals, semiconductors, and insulators to more complex systems such as cryogenically frozen liquids and biological samples. Nevertheless, the fact that field ion evaporation in LAPT is a thermally-triggered process is problematic as many materials are not uniformly heated by the near UV or visible pulsed laser and field evaporation may persist after laser excitation has passed. This results in “thermal tails” that increase background and can complicate identification and resolution of low-concentration species.

Here we present a different approach to LAPT, where instead of using a near-UV laser for inducing a thermal transient, we use an extreme-ultraviolet (EUV) coherent light source to trigger the field-induced ion emission of atoms at the tip's apex, possibly through a mechanism other than a thermal one, such as direct photoionization. The use of EUV photons, with an energy range of 10 - 100 eV, for APT opens the potential for an athermal field ionization pathway. To our knowledge, this process has not been previously observed, but it has been anticipated and described in recent patents.<sup>4,5</sup>

---

Corresponding author's email address: miaja@nist.gov

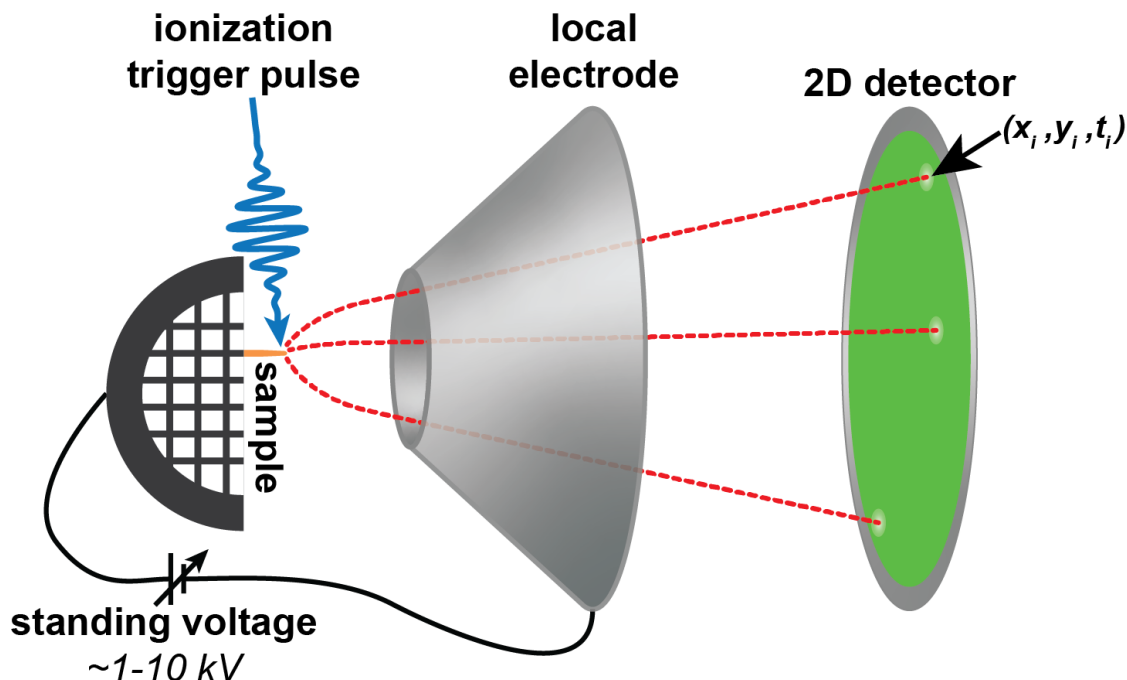


Figure 1. Schematic of the LAPT process. A sample material is shaped into a sharp specimen “tip” with an apex radius typically ranging from 10 – 50 nm. The tip is held at cryogenic temperatures (20 K – 100 K) and electrically biased with a DC standing voltage under ultra-high vacuum conditions. In state-of-the-art conventional laser atom probe, a pulsed, focused laser (typical wavelength 355 nm or 532 nm) is used to induce thermal transients that trigger controlled field ion evaporation from the tip. Each field evaporated ion is accelerated towards the detector where its time-of-flight (TOF) and impact position is recorded. The identities of the ions can be inferred from the TOF data and their origination location can be extracted with back-projection algorithms. The accumulated dataset of TOF and origination position is then used to numerically generate a 3D “reconstruction” of the specimen.

## 2. EXPERIMENTAL SETUP

As previously mentioned, the EUV-pulsed APT developed at NIST is based on the combination of a femtosecond-pulsed coherent EUV light source and a straight flight path atom probe tomograph. Figure 2 shows a schematic representation of our apparatus. There are four essential parts in this system: (1) femtosecond laser, (2) EUV source, (3) vacuum beamline, and (4) atom probe chamber. A more detailed description of this apparatus has been presented by Chiaramonti *et al.*<sup>6</sup>

### 2.1 Femtosecond laser

In our apparatus we use a Ti:Sapphire laser system<sup>7</sup> (Wyvern, KMLabs, Boulder, CO).<sup>\*</sup> This laser delivers 800 nm light with an energy per pulse of  $\sim 1$  mJ and a pulse duration of  $\sim 35$  fs at a repetition rate of 10 kHz.

### 2.2 EUV source

We produce EUV light by means of high-harmonic generation (HHG).<sup>8–10</sup> Through HHG we are able to up-convert the 800 nm (fundamental) light into high harmonics in an Argon-filled hollow core waveguide (XUUS, KMLabs, Boulder, CO). Using an energy per pulse of 0.5 mJ we maximized the HHG process for the 27<sup>th</sup> and 29<sup>th</sup> harmonics, with a respective photon energy of 41.85 eV ( $\lambda \sim 29.6$  nm) and 44.95 eV ( $\lambda \sim 27.6$  nm).

<sup>\*</sup>Identification of specific commercial products or vendors is intended only to adequately describe the experimental conditions. This does not imply endorsement by the National Institute of Standards and Technology. Other vendors, products, or services may be adequate or superior alternatives.

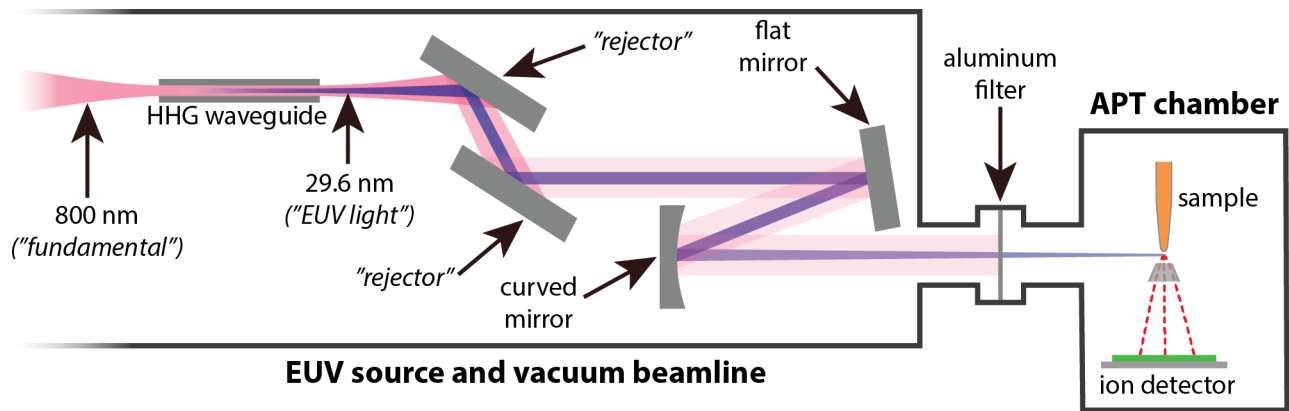


Figure 2. Schematic of the EUV-APT apparatus. The system consists of an amplified Ti:Sapphire laser, an EUV or high-harmonic generation source, a vacuum beamline, and a UHV atom probe chamber. The vacuum beamline includes many individual components, such as infrared-light rejecting optics, a pair of multilayer mirrors, a thin aluminum filter, and multiple vacuum pumps and vacuum gauges.

### 2.3 Vacuum beamline

Since EUV light is strongly absorbed in air, the coupling between the EUV source and the atom probe chamber has to be done under high vacuum conditions. For this reason we designed and constructed a vacuum beamline, whose main purpose is to steer and focus the EUV light into the APT chamber. This beamline includes “rejector” optics that help reflect the EUV light while transmitting (rejecting) the co-propagating 800-nm light. We use a set of custom made multilayer mirrors (one flat and one curved, with a bandwidth of  $\sim 2.4$  eV) to select and focus the 27<sup>th</sup> harmonic into the sample position inside the APT chamber, see Figures 2 and 3. Additionally we have a 200-nm thick Aluminum filter to block the residual 800-nm light and to help maintain a pressure differential between the high-vacuum beamline and the UHV chamber.

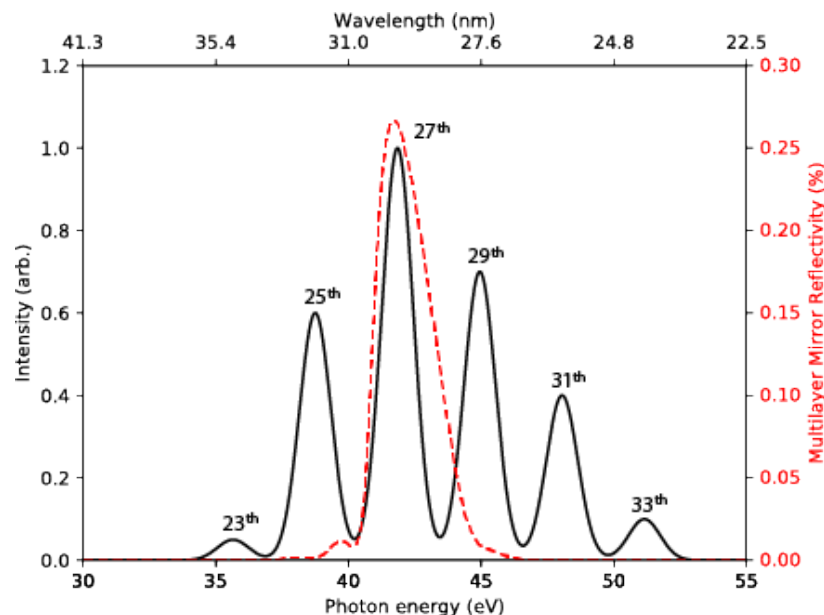


Figure 3. Representative (calculated) HHG spectrum and multilayer mirror (pair) reflectivity curve. The multilayer mirror optics primarily reflect the 27<sup>th</sup> harmonic of the fundamental (41.85 eV; 29.6 nm) with a bandwidth of  $\sim 2.4$  eV.

## 2.4 APT chamber

The APT chamber is a LEAP 3000X-Si Local-electrode straight flight path atom probe tomograph (CAMECA Instruments, Madison, WI). For the development of our apparatus we removed the 532-nm laser and focusing optics that originally came with the APT instrument. Since we are using our own focusing optics and because they are about one meter away from the sample position, our focused EUV spot size at the sample position was calculated to be approximately 50  $\mu\text{m}$ .

## 3. RESULTS, DISCUSSION, AND OUTLOOK

Figure 4 presents some of our initial TOF mass spectra results on a fused silica ( $\text{SiO}_2$ ) tip. The peak assignments were very similar to the ones obtained with conventional LAPT with the silicon peak (doubly ionized) appearing at 14 daltons (Da). The peaks at 16 Da were assigned to single ionized atomic oxygen. Other peaks present in the spectrum are  $\text{O}_2^+$  (32 Da),  $\text{SiO}^+$  (44 Da), and  $\text{SiO}_2^+$  (60 Da). The peaks at 1 and 2 Da are typically assigned to  $\text{H}^+$  and  $\text{H}_2^+$  respectively.

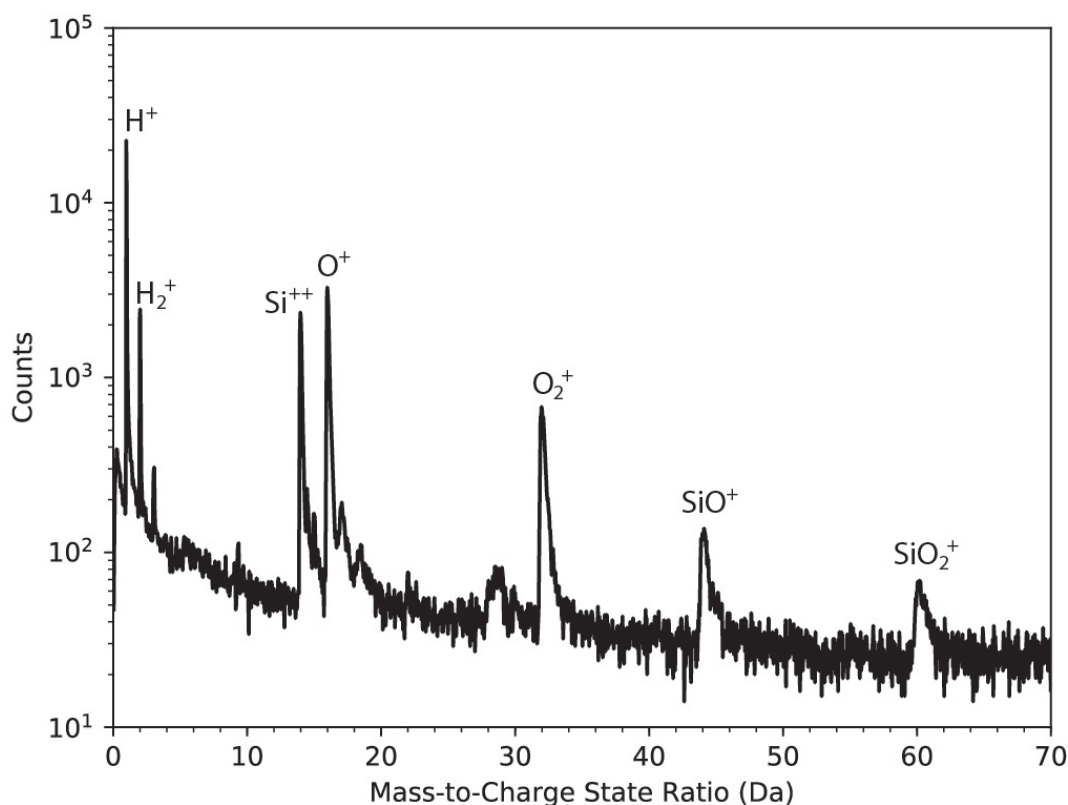


Figure 4. Mass spectrum (without background correction) for an amorphous  $\text{SiO}_2$  specimen using EUV-pulsed atom probe tomography. The peaks at 1 and 2 Da are assigned to  $\text{H}^+$  and  $\text{H}_2^+$  respectively. The peak at 14 Da was assigned to doubly ionized silicon. The peaks at 16 Da were assigned to single ionized atomic oxygen. Other peaks present in the spectrum are  $\text{O}_2^+$  (32 Da),  $\text{SiO}^+$  (44 Da), and  $\text{SiO}_2^+$  (60 Da).

Our results show a decrease in the peak height for some molecular clusters and an apparent reduction of peak tails and widths of the mass spectra peaks when compared to LAPT though the effect of pulse rate and background has not yet been explored. Additionally, the EUV-pulsed APT measurements obtained the correct

specimen composition within the error of the measurement, something that is not always possible in conventional LAPT.<sup>11</sup>

We have also performed EUV-APT measurements on more technologically relevant semiconductor samples, such as gallium nitride (GaN), aluminum gallium nitride (AlGaN), and Mg doped GaN. Recent publications have focused on the study of systematic compositional biases occurring in the atom probe analysis of GaN and AlGaN.<sup>12,13</sup> One of our goals is to examine whether these biases can be minimized or avoided by using EUV light instead of near-UV.

Immediate plans for the further development of this apparatus include: replacing the laser system for one that operates at higher repetition rates, designing an improved vacuum beamline with fewer losses and better focusing conditions, and integrating an EUV beam steering feedback system.

After incorporating these modifications we plan to perform measurements to better understand how the ionization and evaporation processes, happening on the specimen's surface, are affected by the high DC electric field and EUV illumination.

#### 4. SUMMARY

We have adapted an atom probe tomograph with an ultrafast, EUV source in place of a pulsed, visible-UV laser. The apparatus consists of a femtosecond-pulsed laser system, a coherent EUV light source, a vacuum beamline, and a local electrode atom probe tomograph. EUV-assisted field ion evaporation has been demonstrated on various insulating and semiconducting samples. Initial results on fused silica show that the EUV-equipped system might produce mass spectra with fewer complex ions, narrower peaks, and lower background when compared to conventional LAPT performed on the same samples. Our initial results suggest that the field evaporation mechanisms provided by the EUV light may be superior to the strictly thermal mechanism that is generally ascribed to field evaporation of ions in conventional LAPT.

#### ACKNOWLEDGMENTS

We gratefully acknowledge financial support from the NIST Innovations in Measurement Science Program. Material support was provided by CAMECA Instruments, Inc. through a cooperative research and development agreement.

#### REFERENCES

- [1] Kelly, T. F. and Miller, M. K., "Invited Review Article: Atom probe tomography," *Review of Scientific Instruments* **78**(3), 031101 (2007).
- [2] Larson, D., Prosa, T., Ulfing, R., Geiser, B., and Kelly, T., [*Local Electrode Atom Probe Tomography*], Springer, New York (2013).
- [3] Miller, M. and Forbes, R. G., [*Atom-Probe Tomography: The Local Electrode Atom Probe*], Springer, New York (2014).
- [4] Sanford, N. A., Chiamonti, A. N., Gorman, B., and Diercks, D. R., "Hybrid extreme ultraviolet imaging spectrometer," US Patent 9,899,197 (2018).
- [5] Sanford, N. A. and Chiamonti, A. N., "Imaging spectrometer," US Patent 10,153,144 (2018).
- [6] Chiamonti, A. N., Miaja-Avila, L., Blanchard, P. T., Diercks, D. R., Gorman, B. P., and Sanford, N., "A Three-Dimensional Atom Probe Microscope Incorporating a Wavelength-Tuneable Femtosecond-Pulsed Coherent Extreme Ultraviolet Light Source," *MRS Advances* **4**(44-45), 2367–2375 (2019).
- [7] Backus, S., Durfee, C. G., Murnane, M. M., and Kapteyn, H. C., "High power ultrafast lasers," *Review of Scientific Instruments* **69**(3), 1207–1223 (1998).
- [8] Krause, J. L., Schafer, K. J., and Kulander, K. C., "High-order harmonic generation from atoms and ions in the high intensity regime," *Physical Review Letters* **68**(24), 3535–3538 (1992).
- [9] Corkum, P. B., "Plasma perspective on strong field multiphoton ionization," *Physical Review Letters* **71**(13), 1994–1997 (1993).
- [10] Rundquist, A., "Phase-Matched Generation of Coherent Soft X-rays," *Science* **280**(5368), 1412–1415 (1998).

- [11] Mancini, L., Amirifar, N., Shinde, D., Blum, I., Gilbert, M., Vella, A., Vurpillot, F., Lefebvre, W., Lardé, R., Talbot, E., Pareige, P., Portier, X., Ziani, A., Davesne, C., Durand, C., Eymery, J., Butté, R., Carlin, J. F., Grandjean, N., and Rigutti, L., “Composition of wide bandgap semiconductor materials and nanostructures measured by atom probe tomography and its dependence on the surface electric field,” *Journal of Physical Chemistry C* **118**(41), 24136–24151 (2014).
- [12] Russo, E. D., Blum, I., Houard, J., Gilbert, M., Da Costa, G., Blavette, D., and Rigutti, L., “Compositional accuracy of atom probe tomography measurements in GaN: Impact of experimental parameters and multiple evaporation events,” *Ultramicroscopy* **187**, 126–134 (2018).
- [13] Morris, R. J. H., Cuduvally, R., Melkonyan, D., Fleischmann, C., Zhao, M., Arnoldi, L., van der Heide, P., and Vandervorst, W., “Toward accurate composition analysis of GaN and AlGaN using atom probe tomography,” *Journal of Vacuum Science & Technology B, Nanotechnology and Microelectronics: Materials, Processing, Measurement, and Phenomena* **36**(3), 03F130 (2018).